HETEROCYCLES, Vol. 98, No. 3, 2019, pp. 416 - 428. © 2019 The Japan Institute of Heterocyclic Chemistry
Received, 26th January, 2019, Accepted, 22nd February, 2019, Published online, 22nd March, 2019
DOI: 10.3987/COM-19-14048

ONE-POT CASCADE SYNTHESIS OF PYRAZOLE BASED ISOSTERES OF VALDECOXIB BY A [3+2] CYCLOADDITION SEQUENCE AND EVALUATION OF THEIR COX INHIBITORY ACTIVITY

Silvia Roscales,* Nicole Bechmann, Jens Pietzsch, and Torsten Kniess*

Department of Radiopharmaceutical and Chemical Biology, Institute of Radiopharmaceutical Cancer Research, Helmholtz-Zentrum Dresden-Rossendorf, Bautzner Landstraße 400, 01328 Dresden, Germany. E-mail: t.kniess@hzdr.de

Abstract – A series of 5-methyl-3,4-diaryl-substituted 1*H*-pyrazoles, *N*-isosteres of valdecoxib, was synthesized by a [3+2] cycloaddition/[1,5] sigmatropic rearrangement sequence starting from tosylhydrazine, aryl methyl ketones and terminal aryl alkynes bearing various substituents (H, Me, OMe, F, SO_2Me, SO_2NH_2). New pyrazoles were prepared regioselectively in a one-pot process with moderate-good yields. All compounds were used in *in vitro* cyclooxygenase (COX) assays to determine inhibitory potency and selectivity to COX-1 and COX-2. In general, these new pyrazoles are characterized by selective COX-2 inhibition activity in a micromolar range.

INTRODUCTION

Nonsteroidal anti-inflammatory drugs (NSAIDs) are widely used for the treatment of inflammation, fever and pain. The general pharmacological effects of NSAIDs arise from their inhibition of cyclooxygenase (COX) enzymes which catalyze the formation of prostanoids from arachidonic acid. COXs exist as two distinct isoforms, a constitutive form (COX-1) and an inducible form (COX-2), both of which are responsible for the synthesis of prostanoids involved in acute and chronic inflammatory states.[1] Elevated expression of COX-2 has been implicated in manifold pathological events, including chronic inflammatory diseases, coronary heart disease, stroke, and neurodegenerative disorders.[2] It has been also documented recently that COX-2 is overexpressed in many human cancer entities.[3] In consequence, expression of COX-2 has attracted growing attention as a diagnostic marker and therapeutic target in oncology.[4]

The therapeutic actions of nonselective NSAIDs rest upon their inhibition of COX-1 and COX-2; however, the inhibition of COX-1 is accompanied by adverse side effects.[5] In fact, selective COX-2

inhibitors (called coxibs) are more effective and show the advantage of reducing toxicity. In this context, a huge number of compounds based on varying structure classes have been evaluated for selective COX-2 inhibition.[6] Among the structural features, the 5-membered heterocyclic or carbocyclic motif with two vicinal aryl rings attached has evolved as a promising lead structure (Figure 1).[7] It was shown that the sulfonamide or methylsulfonyl group located in *para*-position at one of the phenyl substituents effectively interacts with the COX-2 side pocket through slow tight-binding kinetics.[8] Celecoxib,[9] rofecoxib,[10] and valdecoxib[11] are the most common coxibs, being used, for example, for the treatment of rheumatoid arthritis and osteoarthritis and for the relief of acute pain. However, owing to their adverse cardiovascular side effects and skin reactions, rofecoxib and valdecoxib were later withdrawn from the market.[12] On the other hand parecoxib,[13] a parenterally safe prodrug form of valdecoxib, is still in use for the management and treatment of acute pain. The two pyrazole-containing drugs celecoxib and deracoxib are prominent examples of marketed selective COX-2 inhibitors.[14]

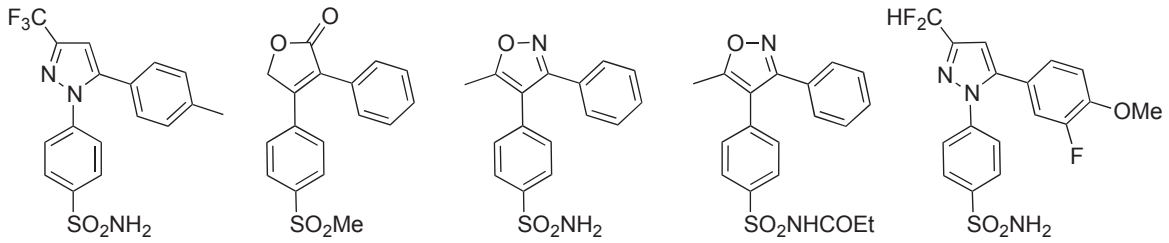

celecoxib **rofecoxib** **valdecoxib** **parecoxib** **deracoxib**

Figure 1

In accordance with our aim of developing new COX-2 inhibitors which are to be generated in a one-pot process, we have recently described the synthesis of a number of novel valdecoxib derivatives by Ru-catalyzed 1,3-dipolar cycloaddition of nitrile oxides with alkynes.[15] Some of the resulting 3,4-diaryl-substituted isoxazoles displayed an affinity in nanomolar range and excellent selectivity towards COX-2. In this line, the replacement of the central isoxazole moiety by a pyrazole ring should lead to new selective COX-2 inhibitors. With this in mind, and in continuation of our 1,3-dipolar cycloaddition approach, we aimed to synthesise novel 3,4-diaryl-substituted pyrazoles **1**, *N*-isosteres of valdecoxib, as potent and selective COX-2 inhibitors (Scheme 1). Accordingly, in this paper we describe the one step synthesis of a series of 5-methyl-3,4-diaryl-1*H*-pyrazoles **1**, by a [3+2] cycloaddition/[1,5] sigmatropic rearrangement sequence. To determine their potential suitability, the COX-1 and COX-2 inhibitory activity of the new compounds was evaluated *in vitro*.

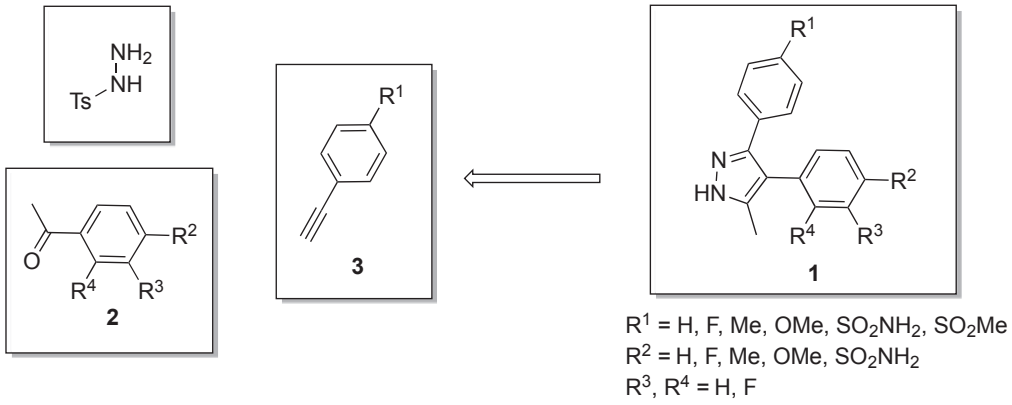

Scheme 1

RESULTS AND DISCUSSION

Chemistry

Pyrazole is an important lead structure in pharmaceutical research, reflected by a great number of pyrazole derivatives present in drugs. The most popular approaches to the synthesis of 3,4,5-trisubstituted pyrazoles are displayed in Scheme 2.[16] They consist of: A) construction of two C-N bonds by condensation of hydrazines with 1,3-dicarbonyl compounds or their 1,3-dielectrophilic synthetic equivalents; B) the generation of one C-N bond and one C-C bond by [3+2] cycloadditions of diazo compounds or other N=N containing dipoles with alkynes and alkenes, respectively. The creation of C-N or C-C bonds by transition-metal-catalyzed cross-coupling reactions of aryl electrophiles with substituted pyrazoles C) is a further general approach. Each method has its own scope and efficiency limitations. Routes based on dipolar cycloaddition reactions usually face regioselectivity problems and are limited by the availability of the diazo compounds, while condensation reaction-based methodologies require multistep routes to yield the pyrazole precursors. In fact, the pyrazole isostere of valdecoxib was synthesized by a six-step procedure starting from commercially available deoxybenzoin.[17]

In recent years it has been shown that tosylhydrazones can be generally employed as educts in the synthesis of diazo compounds from carbonyl compounds.[18] Recently, acetophenone hydrazones[19] and tosylhydrazones[20] were used for the regioselective synthesis of 3,4,5-trisubstituted-1*H*-pyrazoles. In this context, Pérez-Aguilar and Valdés reported a new method for the regioselective preparation of 3,4,5-trisubstituted pyrazoles from readily available *N*-tosylhydrazones and terminal acetylenes through a [3+2] cycloaddition/[1,5] sigmatropic rearrangement sequence (Scheme 2, D).[21] Later, the intramolecular cyclization reaction of *N*-tosylhydrazones/[1,5] with subsequent sigmatropic rearrangement was used for the regioselective synthesis of 5-trifluoromethyl-1*H*-pyrazoles.[22] These results prompted us to evaluate the potential of this reaction sequence as a suitable method for the one-pot generation of 5-methyl-3,4-diaryl-1*H*-pyrazoles **1**, which are not easily available using other methodologies.

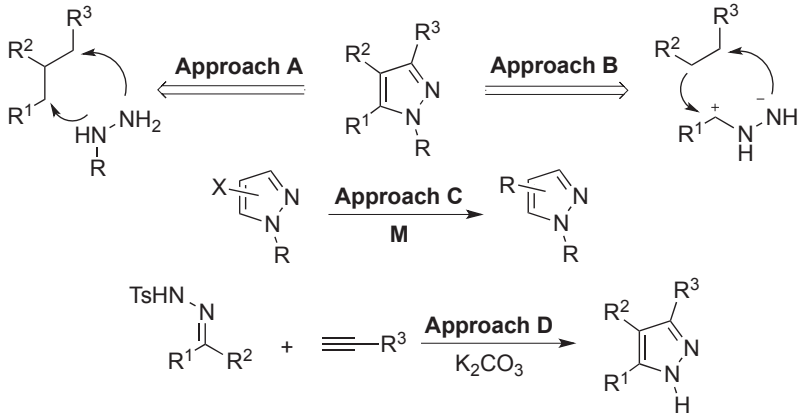

Scheme 2

In an initial experiment, we conducted the reaction between tosylhydrazone **4a** and phenylacetylene **3a** in 1,4-dioxane in the presence of K_2CO_3 at 110 ºC (Scheme 3). The reaction afforded the pyrazole **1a** as a single regioisomer in noticeable 61% yield. Formation of **1a** can be explained by a mechanism that involves the intermediate formation of the diazo compound **5a** from the hydrazine **4a**, followed by [3+2] dipolar cycloaddition with the terminal alkyne **3a** to give a 3*H*-pyrazole and subsequent [1,5] sigmatropic rearrangement and aromatization (Scheme 3, lower part). Only one of the two pyrazole tautomers was observed in ^{1}H NMR spectra; its structure was determined by NOE measurements (NH and Me group).

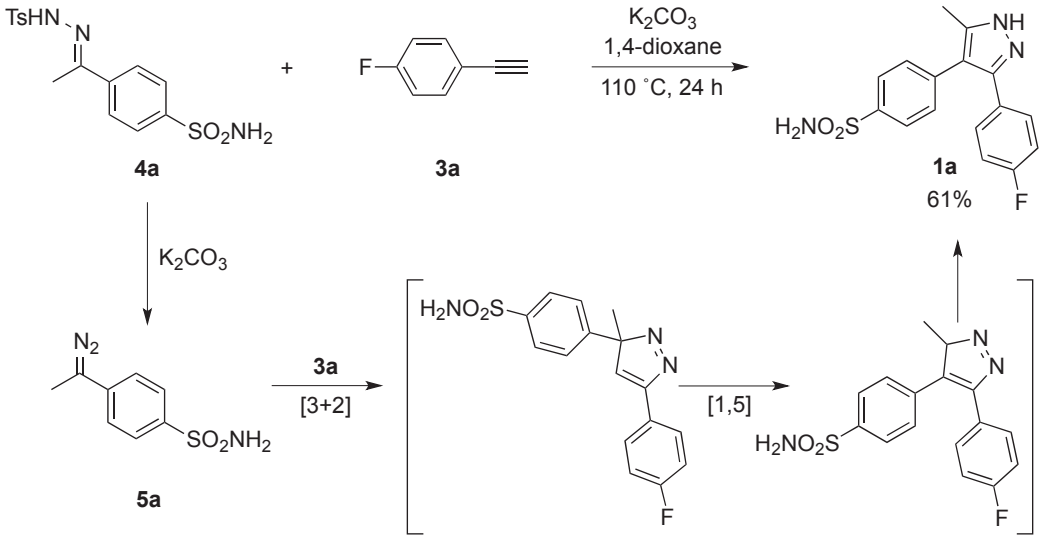

Scheme 3

This initial result prompted us to investigate the scope of this transformation further; after some optimization work, we found that methyl ketones **2** can be easily transformed *in situ* to the corresponding tosylhydrazones **4** by treatment with *p*-toluenesulfonyl hydrazide. After the addition of alkyne **3** and K_2CO_3, 3,4,5-trisubstituted pyrazoles were isolated in good yields in one regioisomeric form. These

one-pot cascade reaction conditions were applied to a set of methyl ketones **2a-i** and terminal alkynes **3a-f**, to form 3,4,5-trisubstituted pyrazoles **1a-k**. The results are summarized in Table 1.

Table 1. Synthesis of diaryl-substituted pyrazoles **1**

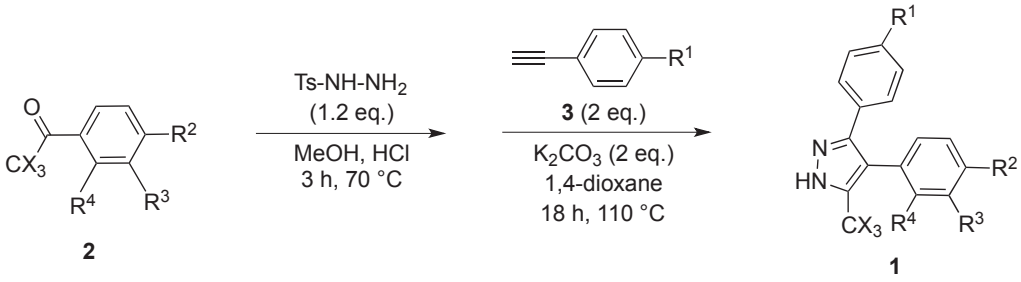

Entry	3, R^1	2, R^2, R^3, R^4, X	1 (Yield, %)
1	**3a**, F	**2a**, SO_2NH_2, H, H, H	**1a** (33)
2	**3b**, H	**2a**, SO_2NH_2, H, H, H	**1b** (31)
3	**3c**, Me	**2a**, SO_2NH_2, H, H, H	**1c** (52)
4	**3d**, OMe	**2a**, SO_2NH_2, H, H, H	**1d** (66)
5	**3e**, SO_2NH_2	**2b**, H, H, H, H	**1e** (42)
6	**3e**, SO_2NH_2	**2c**, F, H, H, H	**1f** (51)
7	**3e**, SO_2NH_2	**2d**, Me, H, H, H	**1g** (82)
8	**3f**, SO_2Me	**2e**, OMe, H, H, H	**1h** (79)
9	**3f**, SO_2Me	**2c**, F, H, H, H	**1i** (70)
10	**3f**, SO_2Me	**2f**, H, F, H, H	**1j** (56)
11	**3f**, SO_2Me	**2g**, H, H, F, H	**1k** (66)
12	**3f**, SO_2Me	**2h**, H, H, H, F	**1l** (0)
13	**3e**, SO_2NH_2	**2h**, H, H, H, F	**1m** (0)
14	**3f**, SO_2Me	**2i**, F, H, H, F	**1n** (0)
15	**3e**, SO_2NH_2	**2i**, F, H, H, F	**1o** (0)

First, the scope of the cascade reaction was evaluated with regard to the structure of the alkyne **3** employing the methyl ketone **2a** possessing the SO_2NH_2 pharmacophore as a substrate (Table 1, entries 1-4). The reaction is general for aromatic-substituted terminal alkynes, bearing electron-donating (entries 3-4) or electron-withdrawing substituents (entry 1). However, in case of the latter a moderate drop in the yield was observed. The reaction with aromatic terminal alkynes bearing SO_2NH_2 **3e** or SO_2Me groups **3f** at *para*-position of the phenyl group also led to the pyrazoles **1e-k** with good yields (entries 5-11). Regarding the structure of the ketone **2**, the process took place efficiently with acetophenone-derived

hydrazones featuring all types of substituents in the aromatic ring. Remarkably, the reaction with electron-donating substituted acetophenones led to the straightforward synthesis of pyrazoles **1g** and **1h** in high yield. The reaction was also successful with a fluorine substituent at *ortho*, *meta* or *para*-position of the aromatic ring (entries 6, 9-11). However, no reaction products were formed with trifluoromethyl ketones as a starting material (entries 12-15). Altogether, these results demonstrate that the cascade synthesis is an excellent method for the preparation of pyrazoles **1** in one pot with high to adequate yields.

***In vitro* COX-1/COX-2 inhibitory activity**

The hitherto unknown inhibitory affinity of **1a-k** towards the COX-1 and COX-2 isoenzyme had to be evaluated. For that purpose, all isolated compounds were subjected to an *in vitro* COX fluorescent inhibitor screening assay where valdecoxib was used as a reference. The resulting *in vitro* enzyme inhibition data, along with the calculated COX-2 selectivity index (COX-2 SI = IC_{50}COX-1/IC_{50}COX-2) of the new pyrazoles **1a-k**, are summarized in Table 2.

Table 2. *In vitro* COX-1 and COX-2 enzyme inhibition data of pyrazoles **1a-k**

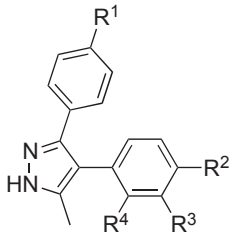

1

Entry	1	R^1	R^2	R^3	R^4	COX-1 IC_{50} (μM)	COX-2 IC_{50} (μM)	COX-2 SI
1	**1a**	F	SO_2NH_2	H	H	>100	8.3	>12.0
2	**1b**	H	SO_2NH_2	H	H	>100	11.4	>8.8
3	**1c**	Me	SO_2NH_2	H	H	>100	18.5	>5.4
4	**1d**	OMe	SO_2NH_2	H	H	>100	91.0	>1.1
5	**1e**	SO_2NH_2	H	H	H	>100	8.0	>12.5
6	**1f**	SO_2NH_2	F	H	H	>100	1.79	>55.9
7	**1g**	SO_2NH_2	Me	H	H	>100	7.1	>14.1
8	**1h**	SO_2Me	OMe	H	H	>100	33.1	>3.0
9	**1i**	SO_2Me	F	H	H	>100	8.22	>12.2
10	**1j**	SO_2Me	H	F	H	>100	2.7	>37.0
11	**1k**	SO_2Me	H	H	F	>100	>100	>1.0
12	valdecoxib					>100	0.05	>2000

All compounds showed no inhibitory potency against COX-1 (>100 μM). Regarding inhibition against COX-2, a more differentiated picture emerged, depending on the substituents of the aromatic rings.

The first series of compounds (**1a-d**, Table 2, entries 1-4) possessing the typical sulfonamide pharmacophore in the *para*-position of the aromatic ring at position 4 of the pyrazole moiety (R^2) showed distinct results of the COX-2 inhibitory activity. With regard to the substituents at the *para*-position of the aryl ring at the position 3 of the pyrazole ring (R^1), it is clearly visible that with increasing size of the substituent the affinity towards COX-2 is reduced. While the H and F substitution pattern is connected with significant but moderate inhibition (8.3-11.4 μM, entries 1-2), large and electron-donating substituents resulted in only weak (Me, entry 3) or almost no inhibition (OMe, entry 4). Accordingly, increasing size and electron-donating properties of the *para*-substituents decrease COX-2 inhibitory potency.

The second series of compounds (**1e-1k**, entries 5-11) possesses the typical sulfonamide or methylsulfonyl COX-2 pharmacophore in the *para*-position of the aromatic ring at position 3 of the pyrazole moiety (R^1 = SO_2NH_2, SO_2Me). Compounds **1e-j** displayed micromolar COX-2 inhibitor activity (entries 5-10), whereas compounds **1f** and **1i** containing an electron-withdrawing fluoro substituent (R^2 = F), behave as the most potent COX-2 inhibitors (IC_{50} = 1.79 μM and 8.22 μM respectively, entries 6, 9). As shown within these results, SO_2NH_2 group as present in **1f** turned out to be a better COX-2 pharmacophore than SO_2Me as present in **1i**. Fluorine-substituted compounds **1f** and **1i** were found to be more potent in comparison with compounds having an electron-donating group **1g** or **1h** (entries 7-8). A *meta*-substituted fluorine at the aryl ring (R^3 = F) (**1j**, entry 10) results in a high observed COX-2 inhibition potency (IC_{50} = 2.7 μM); however, if the fluorine substitution is moved to *ortho* position (R^4 =F) (**1k**, entry 11) no COX-2 inhibition was observed. The structure-activity relationship study of compounds **1e-h** indicated that the order of COX-2 inhibitory potency was F > Me > H > OMe. The order of COX-2 selectivity followed the same chronology. These results suggest that the presence of small, electron-withdrawing substituents like fluorine favors selective inhibition of COX-2. This is in agreement with literature reports which also show a reduced inhibitory potency with increasing size of the *para*-substituent.[23]

Direct comparison of compounds **1a-d** (entries 1-4) and compounds **1e-k** (entries 5-11) further confirms that the *para*-SO_2R-penyl substituent is more favorable at position 3 than at position 4 of the pyrazole moiety regarding COX-2 affinity. Within this series of 3,4,5-trisubstituted pyrazoles, compounds **1f** and **1j** are the most potent and selective COX-2 inhibitors (IC_{50} = 1.79 μM and 2.7 μM) respectively.

A major point of interest and motivation of this study was the question as to whether the substitution of the oxygen by nitrogen (O versus NH) in the five-membered heterocycle in the valdecoxib lead structure would affect the inhibition potency towards COX-2. In Figure 2, valdecoxib, fluoro-substituted

valdecoxib and the corresponding pyrazole derivatives **1b** and **1a**, i.e. valdecoxib NH-isosteres are displayed. It is clearly visible from the IC_{50} values that the COX-2 affinity has significantly dropped by two decimal powers through exchanging the oxazole for a pyrazole moiety. It can be assumed that the free hydrogen on the pyrazole nitrogen interacts with the COX-2 enzyme e.g. via hydrogen bonds and thus prevents a binding with high affinity.[24] Notably, the COX-2 affinity of valdecoxib and its isosteric NH analog is only slightly altered by introduction of a fluorine substituent.

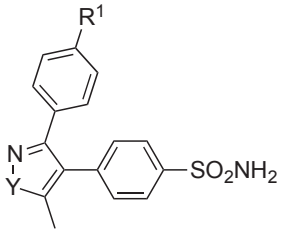

valdecoxib: Y = O, R^1 = H; IC_{50} COX-2 = 0.050 μM[15]
F-valdecoxib: Y = O, R^1 = F; IC_{50} COX-2 = 0.073 μM[15]
1b: Y = NH, R^1 = H; IC_{50} COX-2 = 11.4 μM
1a: Y = NH, R^1 = F; IC_{50} COX-2 = 8.3 μM

Figure 2

EXPERIMENTAL

All commercial reagents and solvents were used without further purification unless otherwise specified. Flash chromatography was conducted using silica gel (mesh size 40-63 μm). Thin-layer chromatography (TLC) was performed on silica gel F-254 aluminium plates. Visualization was carried out using UV (254 nm/366 nm). Analytical HPLC analysis were carried out on an Agilent 1200 system with a C18 column (250 × 4.6 mm, 5 μm) using an isocratic eluent (acetonitrile/water+0.1% TFA 70/30) by a gradient pump with a flow rate of 1 mL/min. The products were monitored by an UV detector at 254 nm. Mass spectrometry was performed with a XevoTQ-S© mass spectrometer by using the electrospray ionization (ESI) mode. Melting points were determined on a melting points apparatus (Galen III) and are uncorrected. Nuclear magnetic resonance spectra (NMR) were recorded on a 400 MHz (Unity INOVA 400, Varian) or 600 MHz (VNMRS 600, Varian) spectrometer. ^{1}H NMR spectra were recorded at 400 MHz, ^{13}C NMR spectra were recorded at 101 MHz, and ^{19}F NMR spectra were recorded at 376 MHz, all of them in $CDCl_3$, $(CD_3)_2SO$ or $CO(CD_3)_2$ solution. NMR spectra were referenced to the residual solvent shifts for ^{1}H and ^{13}C, and to $CFCl_3$ for ^{19}F spectra as internal standards, δ-values are given in ppm.

Starting materials. The alkynes **3f** and **3e** were synthesized by Sonogashira coupling reaction starting from the corresponding aryl bromides by following literature procedures.[15] Tosylhydrazone **4a** was synthesized starting from tosylhydrazine and 4-acetylbenzenesulfonamide by following literature procedure.[25] The rest of compounds are commercially available.

Typical procedure for the synthesis of 3,4-diaryl-5-methyl-1*H*-pyrazoles 1 by [3+2] cycloaddition/[1,5] sigmatropic rearrangement sequence. 4-(3-(4-Fluorophenyl)-5-methyl-1*H*-

pyrazol-4-yl)benzenesulfonamide (1a): Ketone **2a** (50.2 mg, 0.25 mmol, 1.0 equiv.) and *p*-toluensulfonyl hydrazide (56.1 mg, 0.30 mmol, 1.2 equiv.) were dissolved in MeOH (4 mL). A drop of HCl was added to the mixture, which was then refluxed for 3 h. Then, the mixture was cooled to rt and the solvent was evaporated *in vacuo*. To this mixture, the terminal alkyne **3a** (60.3 mg, 0.50 mmol, 2.0 equiv.) and K_2CO_3 (69.4 mg, 0.50 mmol, 2.0 equiv.) were added and the mixture was dissolved in dioxane (4 mL). The system was heated at 110 °C for 12 h. The crude reaction was cooled down to rt, the solvent was eliminated *in vacuo* and a $NaHCO_3$ sat. aq. sol. and AcOEt were added. The layers were separated. The aqueous phase was extracted three times with AcOEt. The combined organic layers were washed with $NaHCO_3$ sat. aq. sol., brine, dried over Na_2SO_4 and filtered. Solvent was removed under reduced pressure. Finally product was purified by flash column chromatography on silica gel (Petrolether:AcOEt 2:8). A white solid; mp 136-138 ºC; IR 3490, 3468, 3021 cm^{-1}; ^1H NMR (400 MHz, DMSO-d_6) δ 12.95 (s, 1H), 7.79 (d, J = 8.3 Hz, 2H), 7.35 (d, J = 8.7 Hz, 6H), 7.16 (s, 2H), 2.24 (s, 3H); ^{13}C NMR (101 MHz, DMSO-d_6) δ 156.50, 144.96, 141.83, 140.56, 137.96, 137.40, 130.30, 129.80, 129.72, 129.60, 129.52, 128.82, 128.52, 127.07, 126.03, 125.89, 125.78, 125.64, 125.47, 125.00, 115.29, 9.78; ^{19}F NMR (376 MHz, DMSO-d_6) δ -114.98. Anal. Calcd for $C_{16}H_{14}FN_3O_2S$; C, 57.99; H, 4.26; N, 12.68. Found: C, 58.13; H, 4.20; N, 12.63.

4-(5-Methyl-3-phenyl-1*H*-pyrazol-4-yl)benzenesulfonamide (1b): A white solid; mp 135-137 ºC; IR 3495, 3470, 3013 cm^{-1}; ^1H NMR (400 MHz, DMSO-d_6) δ 12.93 (s, 1H), 7.78 (d, J = 8.3 Hz, 2H), 7.38 – 7.27 (m, 7H), 2.23 (s, 3H); ^{13}C NMR (101 MHz, DMSO-d_6) δ 141.76, 137.61, 129.81, 128.40, 127.57, 127.47, 125.82, 115.44, 10.07. Anal. Calcd for $C_{16}H_{15}N_3O_2S$; C, 61.32; H, 4.82; N, 13.41. Found: C, 61.45; H, 4.78; N, 13.33.

4-(5-Methyl-3-(*p*-tolyl)-1*H*-pyrazol-4-yl)benzenesulfonamide (1c): A white solid; mp 135-136 ºC; IR 3492, 3466, 3031 cm^{-1}; ^1H NMR (400 MHz, DMSO-d_6) δ 12.88 (s, 1H), 7.77 (d, J = 8.3 Hz, 2H), 7.38 – 7.30 (m, 4H), 7.19 (d, J = 7.8 Hz, 2H), 7.13 (s, 2H), 2.28 (s, 3H), 2.08 (s, 3H); ^{13}C NMR (101 MHz, DMSO-d_6) δ 142.28, 141.66, 140.55, 137.70, 129.77, 127.49, 127.07, 125.79, 125.77, 125.63, 125.46, 25.81, 14.95. Anal. Calcd for $C_{17}H_{17}N_3O_2S$; C, 62.36; H, 5.23; N, 12.83. Found: C, 62.46; H, 5.21; N, 12.75.

4-(3-(4-Methoxyphenyl)-5-methyl-1*H*-pyrazol-4-yl)benzenesulfonamide (1d): A white solid; mp 145-147 ºC; IR 3488, 3470, 3030 cm^{-1}; ^1H NMR (400 MHz, DMSO-d_6) δ 12.82 (s, 1H), 7.77 (d, J = 8.3 Hz, 2H), 7.34 (m, 4H), 7.23 (d, J = 8.7 Hz, 2H), 6.89 (s, 2H), 3.74 (s, 2H), 2.21 (s, 3H); ^{13}C NMR (101 MHz, DMSO-d_6) δ 154.20, 151.05, 141.62, 137.79, 129.76, 129.24, 128.81, 125.80, 125.31, 122.50, 55.07, 10.91. Anal. Calcd for $C_{17}H_{17}N_3O_3S$: C, 59.46; H, 4.99; N, 12.24. Found: C, 59.33; H, 4.95; N, 12.29.

4-(5-Methyl-4-phenyl-1*H*-pyrazol-3-yl)benzenesulfonamide (1e): A white solid; mp 151-153 ºC; IR

3490, 3469, 3012 cm^{-1}; ^1H NMR (400 MHz, DMSO-d_6) δ 12.98 (s, 1H), 7.70 (d, J = 8.1 Hz, 2H), 7.48 (d, J = 7.9 Hz, 2H), 7.43 – 7.34 (m, 2H), 7.35 – 7.26 (m, 3H), 7.22 – 7.15 (m, 2H), 2.22 (s, 3H); ^{13}C NMR (101 MHz, DMSO-d_6) δ 147.20, 142.78, 137.94, 133.90, 130.13, 129.06, 127.92, 127.05, 126.02, 117.58, 10.05. Anal. Calcd for $C_{16}H_{15}N_3O_2S$; C, 61.32; H, 4.82; N, 13.41. Found: C, 61.21; H, 4.84; N, 13.45.

4-(4-(4-Fluorophenyl)-5-methyl-1*H*-pyrazol-3-yl)benzenesulfonamide (1f): A white solid; mp 150-152 ºC; IR 3483, 3461, 3023 cm^{-1}; ^1H NMR (300 MHz, acetone-d_6) δ 12.20 (s, 1H), 7.79 (d, J = 8.5 Hz, 2H), 7.57 (d, J = 8.5 Hz, 2H), 7.27 (dd, J = 8.7, 5.5 Hz, 2H), 7.17 (t, J = 8.8 Hz, 2H), 6.57 (s, 2H), 2.28 (s, 3H); ^{13}C NMR (75 MHz, acetone-d_6) δ 162.66 (d, J = 243.8 Hz), 143.56, 138.05, 132.77, 132.67, 131.02, 130.97, 128.50, 126.86, 117.73, 116.25 (d, J = 21.5 Hz), 10.29; ^{19}F NMR (282 MHz, acetone-d_6) δ -117.62. Anal. Calcd for $C_{16}H_{14}FN_3O_2S$; C, 57.99; H, 4.26; N, 12.68. Found: C, 58.10; H, 4.27; N, 12.63.

4-(5-Methyl-4-(*p*-tolyl)-1*H*-pyrazol-3-yl)benzenesulfonamide (1g): A white solid; mp 150-152 ºC; IR 3481, 3455, 3019 cm^{-1}; ^1H NMR (400 MHz, DMSO-d_6) δ 12.94 (s, 1H), 7.71 (d, J = 8.0 Hz, 2H), 7.49 (d, J = 7.7 Hz, 2H), 7.30 (s, 2H), 7.19 (d, J = 7.9 Hz, 2H), 7.07 (d, J = 8.1 Hz, 2H), 2.33 (s, 3H), 2.20 (s, 3H); ^{13}C NMR (101 MHz, DMSO-d_6) δ 146.70, 142.32, 137.59, 135.69, 130.38, 129.54, 129.23, 127.42, 125.57, 117.03, 20.75, 9.57. Anal. Calcd for $C_{17}H_{17}N_3O_2S$: C, 62.36; H, 5.23; N, 12.83. Found: C, 62.25; H, 5.20; N, 12.89.

4-(4-Methoxyphenyl)-5-methyl-3-(4-(methylsulfonyl)phenyl)-1*H*-pyrazole (1h): A white solid; mp 137-139 ºC; IR 3470, 3067 cm^{-1}; ^1H NMR (400 MHz, DMSO-d_6) δ 12.98 (s, 1H), 7.82 (d, J = 7.9 Hz, 2H), 7.59 (d, J = 8.1 Hz, 2H), 7.12 (d, J = 8.6 Hz, 2H), 6.96 (d, J = 8.6 Hz, 2H), 3.78 (s, 3H), 3.20 (s, 3H), 2.18 (s, 3H); ^{13}C NMR (101 MHz, DMSO-d_6) δ 158.07, 130.85, 127.47, 126.91, 125.30, 114.16, 55.00, 43.40, 10.66. Anal. Calcd for $C_{18}H_{18}N_2O_3S$; C, 63.14; H, 5.30; N, 8.18. Found: C, 63.06; H, 5.32; N, 8.23.

4-(4-Fluorophenyl)-5-methyl-3-(4-(methylsulfonyl)phenyl)-1*H*-pyrazole (1i): A white solid; mp 130-132 ºC; IR 3474, 3045 cm^{-1}; ^1H NMR (300 MHz, $CDCl_3$) δ 7.73 (d, J = 8.3 Hz, 2H), 7.52 (d, J = 8.3 Hz, 2H), 7.17 – 6.88 (m, 4H), 3.04 (s, 3H), 2.16 (s, 3H); ^{13}C NMR (75 MHz, $CDCl_3$) δ 162.13 (d, J = 246.8 Hz), 148.28, 143.84, 142.05, 139.24, 138.47, 131.69 (d, J = 7.9 Hz), 129.84, 128.79, 128.48, 127.62, 119.06, 117.89, 115.94 (d, J = 21.4 Hz), 44.56, 10.42; ^{19}F NMR (376 MHz, DMSO-d_6) δ -115.14. Anal. Calcd for $C_{17}H_{15}FN_2O_2S$; C, 61.80; H, 4.58; N, 8.48. Found: C, 61.70; H, 4.61; N, 8.48.

4-(3-Fluorophenyl)-5-methyl-3-(4-(methylsulfonyl)phenyl)-1*H*-pyrazole (1j): A white solid; mp 131-133 ºC; IR 3467, 3025 cm^{-1}; ^1H NMR (400 MHz, DMSO-d_6) δ 13.12 (s, 1H), 7.84 (d, J = 7.9 Hz, 2H), 7.58 (d, J = 8.0 Hz, 2H), 7.43 (td, J = 7.9, 6.3 Hz, 1H), 7.21 – 7.10 (m, 1H), 7.05 (d, J = 10.1 Hz, 1H), 7.01 (dd, J = 7.6, 1.2 Hz, 1H), 3.21 (s, 3H), 2.23 (s, 3H); ^{13}C NMR (101 MHz, DMSO-d_6) δ 162.21 (d, J = 243.8 Hz), 139.21, 138.25, 135.82 (d, J = 8.2 Hz), 130.57 (d, J = 8.8 Hz), 125.96 (d, J = 2.6 Hz),

116.24 (d, J = 21.0 Hz), 113.55 (d, J = 20.8 Hz), 43.39, 9.56; ^{19}F NMR (376 MHz, DMSO-d_6) δ -114.72. Anal. Calcd for $C_{17}H_{15}FN_2O_2S$; C, 61.80; H, 4.58; N, 8.48. Found: C, 61.73; H, 4.60; N, 8.50.

4-(2-Fluorophenyl)-5-methyl-3-(4-(methylsulfonyl)phenyl)-1*H*-pyrazole (1k): A white solid; mp 131-132 ºC; IR 3467, 3020 cm^{-1}; ^{1}H NMR (400 MHz, DMSO-d_6) δ 13.16 (s, 1H), 7.81 (d, J = 8.1 Hz, 2H), 7.57 (d, J = 8.1 Hz, 2H), 7.48 – 7.38 (m, 1H), 7.33 – 7.23 (m, 3H), 3.19 (s, 3H), 2.08 (s, 3H); ^{13}C NMR (101 MHz, DMSO-d_6) δ 159.50 (d, J = 244.3 Hz), 146.88, 146.50, 139.15, 138.90, 138.85, 132.45 (d, J = 3.1 Hz), 129.61 (d, J = 8.1 Hz), 127.78, 127.00, 126.99, 126.82, 124.76 (d, J = 3.5 Hz), 120.85 (d, J = 16.1 Hz), 115.90 (d, J = 22.2 Hz), 110.65, 43.40, 9.42; ^{19}F NMR (376 MHz, DMSO-d_6) δ -113.87. Anal. Calcd for $C_{17}H_{15}FN_2O_2S$; C, 61.80; H, 4.58; N, 8.48. Found: C, 61.94; H, 4.55; N, 8.44.

COX inhibition assay: COX-1 and human COX-2 was determined using the fluorescence-based COX assay "COX Fluorescent Inhibitor Screening Assay KIT" (catalogue number 700100; Cayman Chemicals, USA) according to manufacturer's instructions. All compounds were assayed in a concentration range of 0.01-100 μM. Two technical replicates were performed for each inhibitor concentration. The mean of these two values was used for estimating the IC_{50} values using a nonlinear fitting procedure (sigmoidal dose-response model) with Origin® Software.

ACKNOWLEDGEMENTS

The excellent technical assistance of Johanna Pufe and Mareike Barth in performing COX inhibitory assays is greatly acknowledged. Constantin Mamat and Reik Löser are acknowledged for recording the Nuclear Magnetic Resonance Spectra. Silvia Roscales is grateful for a post-doctoral fellowship from Ramón Areces Foundation (2015-2016).

REFERENCES AND NOTES

1. (a) F. A. Fitzpatrick, *Curr. Pharm. Des.*, 2004, **10**, 577; (b) R. G. Kurumbail, J. R. Kiefer, and L. J. Marnett, *Curr. Opin. Struct. Biol.*, 2001, **11**, 752; (c) L. J. Marnett, *Curr. Opin. Chem. Biol.*, 2000, **4**, 545; (d) D. L. Simmons, R. M. Botting, and T. Hla, *Pharmacol. Rev.*, 2004, **56**, 387.
2. E. Cudaback, N. L. Jorstad, Y. Yang, T. J. Montine, and C. D. Keene, *Biochem. Pharmacol.*, 2014, **88**, 565.
3. B. B. Aggarwal, B. Sung, and S. C. Gupta, 'Inflammation and Cancer,' Adv Exp Med Biol, Springer, Basel, 2014.
4. (a) M. Laube, T. Kniess, and J. Pietzsch, *Antioxidants*, 2016, **5**, 14; (b) E. Yiannakopoulou, *Eur. J. Cancer Prev.*, 2015, **24**, 416; (c) J. L. Liggett, X. Zhang, T. E. Eling, and S. J. Baek, *Cancer Lett.*, 2014, **346**, 217; (d) M. Laube, T. Kniess, and J. Pietzsch, *Molecules*, 2013, **18**, 6311.
5. M. E. Turini and R. N. DuBois, *Annu. Rev. Med.*, 2002, **53**, 35.

6. P. Singh and A. Mittal, *Mini-Rev. Med. Chem.*, 2008, **8**, 73.
7. J. J. Talley, *Prog. Med. Chem.*, 1999, **36**, 201.
8. (a) M. C. Walker, R. G. Kurumbail, J. R. Kiefer, K. T. Moreland, C. M. Koboldt, P. C. Isakson, K. Seibert, and J. K. Gierse, *Biochem. J.*, 2001, **357**, 709; (b) R. G. Kurumbail, A. M. Stevens, J. K. Gierse, J. J. McDonald, R. A. Stegeman, J. Y. Pak, D. Gildehaus, J. Miyashiro, T. D. Penning, K. Seibert, P. C. Isakson, and W. C. Stallings, *Nature*, 1996, **384**, 644.
9. D. Clemett and K. L. Goa, *Drugs*, 2000, **59**, 957.
10. A. J. Matheson and D. P. Figgitt, *Drugs*, 2001, **61**, 833.
11. D. Ormrod, K. Wellington, and A. J. Wagstaff, *Drugs*, 2002, **62**, 2059.
12. J.-M. Dogné, C. T. Supuran, and D. Pratico, *J. Med. Chem.*, 2005, **48**, 2251.
13. D. L. Teagarden and S. Nema, 'Prodrugs Biotechnology: Pharmaceutical Aspects,' Vol. 5, ed. by V. J. Stella, R. T. Borchardt, M. J. Hagemann, R. Oliyai, H. Maag, and J. Tilley, Springer, 2007, pp. 1335–1346.
14. S. M. Sakya, H. Cheng, K. M. Lundy DeMello, A. Shavnya, M. L. Minich, B. Rast, J. Dutra, C. Li, R. J. Rafka, D. A. Koss, J. Li, B. H. Jaynes, C. B. Ziegler, D. W. Mann, C. F. Petras, S. B. Seibel, A. M. Silvia, D. M. George, A. Hickman, M. L. Haven, and M. P. Lynch, *Bioorg. Med. Chem. Lett.*, 2006, **16**, 1202.
15. (a) S. Roscales, N. Bechmann, D. Holger Weiss, M. Köckerling, J. Pietzsch, and T. Kniess, *Med. Chem. Commun.*, 2018, **9**, 534; (b) S. Roscales and T. Kniess, *J. Labelled Compd. Radiopharm.*, 2019, 1.
16. (a) S. Fustero, M. Sánchez-Roselló, P. Barrio, and A. Simón-Fuentes, *Chem. Rev.*, 2011, **111**, 6984; (b) A. Schmidt and A. Dreger, *Curr. Org. Chem.*, 2011, **15**, 1423; (c) J. Elguero, A. M. S. Silva, and A. C. Tom 'Modern Heterocyclic Chemistry,' Vol. 2, ed. by J. Alvarez-Builla, J. J. Vaquero, and J. Barluenga, Wiley-VCH, Weinheim, 2011, pp. 635–725.
17. G. Szabó, J. Fischer, and Á. Kis-Varga, *Pharmazie*, 2006, **61**, 522.
18. (a) Z. Shao and H. Zhang, *Chem. Soc. Rev.*, 2012, **41**, 560; (b) J. Barluenga and C. Valdés, *Angew. Chem. Int. Ed.*, 2011, **50**, 7486; (c) J. R. Fulton, V. K. Aggarwal, and J. de Vicente, *Eur. J. Org. Chem.*, 2005, 1479.
19. R. Vanjari, T. Guntreddi, S. Kumar, and K. N. Singh, *Chem. Commun.*, 2015, **51**, 366.
20. (a) S. Panda, P. Maity, and D. Manna, *Org. Lett.*, 2017, **19**, 1534; (b) W. Liu, H. Wang, H. Zhao, B. Li, and S. Chen, *Synlett*, 2015, 2170; (c) W.-L. Wang, Y.-L. Feng, W.-Q. Gao, X. Luo, and W.-P. Deng, *RSC Adv.*, 2013, **3**, 1687.
21. M. C. Pérez-Aguilar and C. Valdés, *Angew. Chem.*, 2013, **125**, 7360.
22. Q. Sha, H. Liu, and Y. Wei, *Eur. J. Org. Chem.*, 2014, 7707.

23. B. Portevin, C. Tordjman, P. Pastoureau, J. Bonnet, and G. De Nanteuil, *J. Med. Chem.*, 2000, **43**, 4582.
24. Analysis of binding affinities for celecoxib analogues with COX-2 from combined Docking and Monte Carlo Simulations showed that ligands that contain hydrogen-bonding functionality are poor binders. M. L. Plount Price and W. L. Jorgensen, *J. Am. Chem. Soc.*, 2000, **122**, 9455.
25. Y. Huang, X. Li, X. Wang, Y. Yu, J. Zheng, W. Wu, and H. Jiang, *Chem. Sci.*, 2017, **8**, 7047.